Thermodynamic analysis of a thermoacoustic travelling wave engine

Adam RUZIEWICZ, Alexander KRUSE, Zbigniew GNUTEK

DOI: 10.30464/jmee.2018.2.1.67
Online: http://www.jmee.tu.koszalin.pl/download_article/jmee_2018_01_067074.pdf

Cite this article as:
Ruziewicz A., Kruse A., Gnutek Z. Thermodynamic analysis of a thermoacoustic travelling wave engine. Journal of Mechanical and Energy Engineering, Vol. 2(42), No. 1, 2018, pp. 67-74.

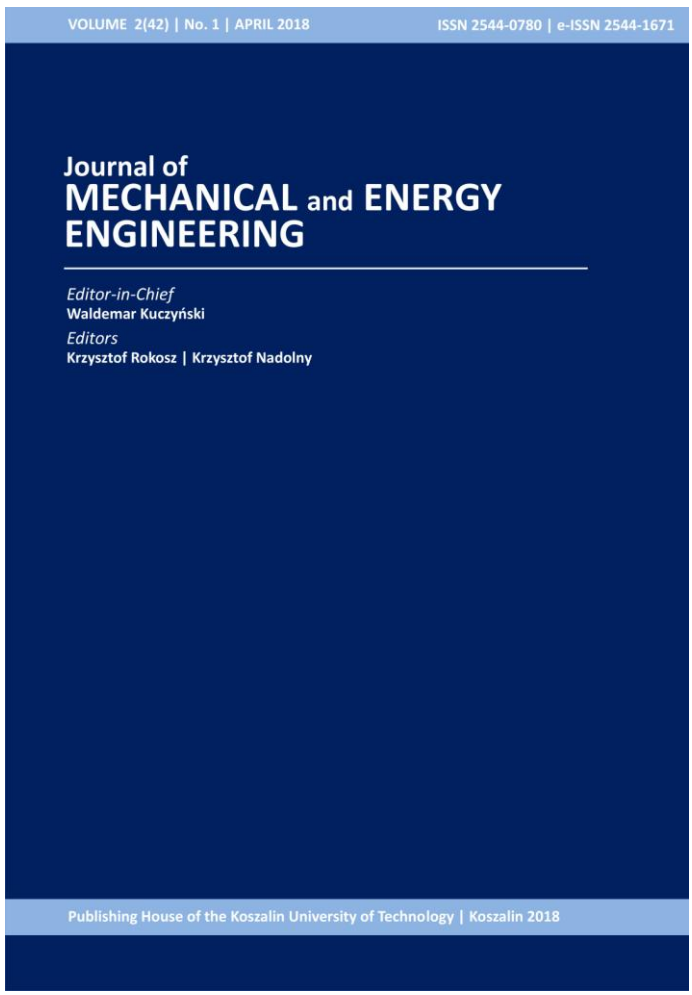

Journal of Mechanical and Energy Engineering

ISSN (**Print**): 2544-0780
ISSN (**Online**): 2544-1671
Volume: 2(42)
Number: 1
Year: 2018
Pages: 67-74

Article Info:
Received 20 February 2018
Accepted 20 March 2018

Journal of
MECHANICAL and ENERGY
ENGINEERING

ISSN: 2544-0780 | e-ISSN: 2544-1671
Vol. 2(42) | No. 1 | April 2018 | pp. 67-74
DOI: 10.30464/jmee.2018.2.1.67

THERMODYNAMIC ANALYSIS OF A THERMOACOUSTIC TRAVELLING WAVE ENGINE

Adam RUZIEWICZ[1*], Alexander KRUSE[2], Zbigniew GNUTEK[1]

[1*] Department of Thermodynamics, Theory of Machines and Thermal Systems, Faculty of Mechanical and Power Engineering, Wroclaw University of Science and Technology, Wybrzeze Wyspianskiego 27, 50-370 Wrocław, Poland, e-mail: adam.ruziewicz@pwr.edu.pl
[2] Institute of Aerospace Engineering, TU Dresden, 01062 Dresden, Germany

(Received 20 February 2018, Accepted 20 March 2018)

Abstract: Thermoacoustics has become a promising technology to use heat from low temperature sources to drive engines. This study proposes a single-stage thermoacoustic travelling-wave engine for waste-heat recovery at 150°C. All the construction details of such a system are provided. A recently developed configuration of a looped tube with an impedance matching side-branch stub is proposed. A numerical model of the engine is built in DeltaEC software to conduct the simulations. Furthermore, a detailed thermodynamic analysis of the engine is presented, including an energy balance, a description of the basic acoustic parameters in a steady state, as well as a study of a variable load influence on the performance of the engine. The Authors pointed out the necessity of the engine optimization and a proper choice of load related acoustic impedance, which would consider a trade-off between high power and high efficiency. Eventually, a possibility of achieving 40% exergy efficiency of the proposed engine is confirmed.

Keywords: thermoacoustic engine, Stirling cycle, waste energy, energy conversion

1. INTRODUCTION

Thermoacoustics is a fairly new promising technology, one which may be used for waste heat recovery. The thermoacoustic effect leads to energy conversion from heat to acoustic power or vice-versa. Its main application areas are heat-driven engines and refrigerators [1]. Thermoacoustic technology has many assets, i.e. simple construction devices, no moving parts (within the converter), the usage of environment-friendly gases and possibility of the usage of cryogenic temperature heat sources. In spite of wide interest in thermoacoustics on the part of many research teams around the world, this technology is still in the phase of investigation and prototypes construction.

Ceperley [2] first recognized that a travelling wave passing through an isothermal regenerator results in a reversible Stirling thermodynamic cycle and, by extension, an acoustic power gain. He defined similarities between the gas motion induced by an acoustic wave and pistons movements in a conventional Stirling engine. A travelling-wave thermoacoustic engine is known as a thermoacoustic Stirling engine but in this case the acoustic wave oscillation acts in a similar fashion as mechanical pistons which cause the demanded gas motion.

The second important finding made by Ceperley is the fact that high viscous losses in the regenerator can be reduced by a local enhancement of acoustic impedance [3]. However, the first running travelling-wave thermoacoustic engine was constructed in 1998 by Yazaki et al. [4]. Thereon Backhaus and Swift [5] proposed a different torus shape of an engine with a side-branch resonator maintaining high impedance and proper travelling wave conditions within the regenerator. Tijani and Spoelstra [6] as well as Haberbusch [7] improved some construction details reaching up to 52% exergetic efficiency. Nevertheless, engines of such configurations need a high temperature difference to start, and they only reach the maximum efficiency by a heat source temperature of ca. 600-725°C.

To be economically worthwhile and competitive to conventional devices, thermoacoustic engines should sustain high exergetic efficiency even by the onset temperature of 70-200°C, which is the typical range

for low-temperature waste heat sources [8,9]. A recently investigated looped-tube type of thermoacoustic devices can meet these demands.

In such an engine, high local impedance is maintained by enlarging the cross-sectional area of the thermoacoustic core (the regenerator and accompanying heat exchangers) placed in the looped acoustic feedback tube, what was pointed out by Ceperley [3] and firstly carried out by de Blok [8]. In this way, operating and onset temperatures were significantly decreased. Continuing this research, the usage of multiple thermoacoustic cores placed in one acoustic loop was proposed. In his four-stage travelling-wave engine driven from a heat source of temperature 150 °C, an exergetic efficiency of 40% was achieved [10]. This type of engines makes thermoacoustic technology applicable for low-grade heat sources such as solar heat.

In their numerical analysis, Zhang et al. [9,11] pointed out that stage number in the engine has to be optimized after considering a trade-off between working temperature difference and the system performance. This means that an engine with fewer stages can perform better for little higher temperatures. Fewer stages could be also preferable, regarding a simplification of the construction and production costs.

In the present paper, a single-stage travelling-wave engine driven by a heat source at 150 °C is analyzed. In the chapters to follow, the construction details and a numerical model of the engine and demands for acoustic conditions are presented. In addition, an extensive energy balance of the analyzed operational state of the engine is carried out.

2. MATHEMATICAL MODEL

The numerical calculations of the working parameters of the thermoacoustic engine, as well as an analysis of variable external parameters was carried out in DeltaEC software [12] developed by Los Alamos Laboratory. The program solves numerically one-dimensional wave equation for given geometry and working gas parameters including a thermoacoustic effect, according to the linear thermoacoustic theory [1]. A model is described by built-up segments, such as: waveguide (pipe), heat exchangers, regenerator, etc. which are connected in one common acoustic network.

2.1. Thermoacoustic engine construction

A schematic drawing of the thermoacoustic looped tube engine analysed is shown in Fig.1. The basic elements comprising a whole system are described below.

A heart of the engine is the thermoacoustic core, which consists of an ambient heat exchanger (AHX), a hot heat exchanger (HHX) and a regenerator (REG) sandwiched in between. Heat is supplied to the engine in HHX and released in AHX, which induces a temperature gradient over the REG.

The feedback tube (FBT) is a pipe with a diameter of 12.6 cm which forms a loop and enables an acoustic wave to travel back to the core. The core diameter is much larger than FBT and the ratio of their areas amounts to 10.

There are two side-branched pipes along the FBT. The first one, to the right, forms the core, denotes an acoustic load, where acoustic power leaves the system. The second one is a stub, which plays a role of an acoustic field tuner.

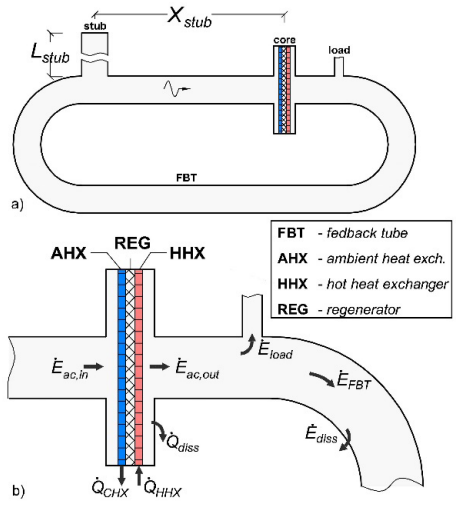

Fig. 1. Scheme of the thermoacoustic engine analyzed; (a) whole engine model; (b) detailed view on thermoacoustic core and the load with pointed out energy fluxes

Tab. 1. Construction details of the engine

Construction details		
Heat exchangers		
length	15	mm
porosity	70	%
hydraulic radius	0.6	mm
Regenrator		
length	20	mm
porosity	80	%
hydrauclic radius	54.8	µm
Stub		
position	86.8	cm
length	65.6	cm
Others		
feedback length	4	m
feedback diameter	12.6	cm
core diameter	40	cm

The main construction details of the engine are presented in Table 1. Both heat exchangers (AHX and HHX) have a simple parallel plate construction, commonly used in car radiators. This type is very often used in thermoacoustic devices, too. The hydraulic radius of the heat exchangers is equal to 0.6 mm and porosity (free area fraction) is 70%, which assures a good thermal contact with the gas. A fin (plate) is only 15 mm long, which is already more than gas peak-to-peak displacement. This means that longer heat exchangers would not supply (release) more heat to the engine in these particular conditions. REG is a 20mm long stack of stainless steel mesh screens with a hydraulic radius of 54.8μm and a porosity of 80%. The whole core section with the enlarged diameter of 40 cm takes only 10 cm of 4 m long loop.

The stub is a side-branched pipe of the same diameter as FBT, which tunes the proper acoustic conditions in REG. By changing its length and position, the relevant acoustic parameters in REG (the impedance ratio and the phase difference between the oscillating pressure and velocity) can be widely adjusted. The values determined of normalized impedance Z_n=8 and phasing φ=-20° are reached by a particular stub arrangement. Its position X_{stub} is 0.868 m from the centre of REG and its length L_{stub} is 0.656 m. In the model, the values of Z_n and φ are defined as boundary conditions and the geometry of the stub is a result of numeric calculations, depending on all the acoustic field parameters.

Tab. 2. Engine parameters

Acoustic parameters		
Normalized impedance	8	
Phasing	-20	°
Load impedance	2.705	MPa s/m^3
Efficiency	10	%
Outer parameters		
Gas type	helium	
Gas mean pressure	3	MPa
Heater temperature	150	°C
Cooler temperature	15	°C

The load of the engine is represented in the model by a complex acoustic impedance. A ratio between its value and FBT impedance decides how much acoustic power could leave the system and drive an external load (the alternator, the turbine). In the basic state of the model, the real part of impedance Re[Z_{load}] amounts to 2,7MPa·s/m^3, and its imaginary part Im[Z_{load}] equals 0.

Heat is supplied in the HHX at the temperature of 150°C and it is released in the AHX at 15°C. The working gas is helium under mean pressure of 30 bar. The resonance frequency of the system under these conditions is 214.5 Hz. All the above-mentioned parameters are collected in Table 2.

2.2. Acoustic conditions in the regenerator

In the linear theory of thermoacoustics, generated acoustic power $d\dot{E}$ in a length of the regenerator dx is defined as [1]:

$$\frac{\mathrm{d}\dot{\mathrm{E}}}{\mathrm{dx}} = -\frac{r_v}{2}\left|U_1\right|^2 + \frac{1}{2}\mathrm{Re}[g]\cdot\cos(\varphi)\cdot\left|p_1\right|\cdot\left|U_1\right|\cdot \quad (1)$$

The first element on the right side of Equation (1) defines acoustic losses due to the viscous resistance per length r_v. The second one represents acoustic power generated in the regenerator, where g is the gain factor and $|p_1|$, $|U_1|$ are amplitudes of pressure and volume flow rate oscillations. According to Equation (1), acoustic wave must fulfil two requirements [5]:

(1) φ should be close to 0° to ensure a reversible thermodynamic cycle and maximize the second term of the equation (φ=0° characterise a travelling-wave and φ=90° - a standing-wave). In reality, an optimum value depends on the whole acoustic field and it usually differs from 0.

(2) |U1| has to be small in order to reduce acoustic losses defined by the first term of Equation (1). Considering viscous resistance r_v, it is the velocity v_1 that is rather responsible for losses. Velocity is equal to $v_1=U_1/A$ and it can be easily reduced by enlarging cross-sectional area A.

A commonly used factor, which characterises acoustic conditions in the REG, is normalised impedance Z_n. Z_n is a ratio between specific acoustic impedance and the gas characteristic impedance, which is a product of density ρ_m and speed of sound a:

$$Z_n = \left|\frac{p_1}{v_1}\right| \cdot \frac{1}{\rho_m a}. \quad (2)$$

In order to ensure proper conditions in the REG and to decrease losses, Z_n should be much bigger than 1. Its different values depend mostly on the acoustic system and they varie in the range of 5-30. However a local increase of impedance causes acoustic wave reflections that are responsible for disturbances (standing-wave components) of travelling wave propagating in a waveguide. Introducing a “matched” impedance at another spot of the FBT may compensate for these disturbances and allow reaching the demanded acoustic conditions. This additional impedance can be brought in by a side-branch stub. By changing its length and position, acoustic conditions in the REG can be easily tuned within a wide scale. In the general position of a stub is close.

A more detailed analysis of normalized impedance and phasing on the engine performance as well as

research on other important construction parameters done by the authors has been published in [18].

2.3. Acoustic load of an engine

In order to use acoustic power generated in the engine, it has to be converted into a more useful form. One possibility is to transform it into electric power. This can be done by commonly used linear alternators [13-16] or a recently developed bi-directional turbine [17]. Furthermore, a thermoacoustic heat pump can be introduced to the loop as a load. In this combined system (engine – heat pump), energy is first converted in the engine stage from thermal to acoustic and then in the heat pump stage back from acoustic to thermal, but at a different temperature level. Such a system could be used as a refrigerator driven by waste-heat.

Any load introduced to the system can be characterized by complex acoustic impedance, which on the one hand allows the removal of acoustic power from the thermoacoustic system but on the other hand it also affects the whole acoustic field in the engine. Its value is described by the real and imaginary part of load impedance, $Re[Z_{load}]$ and $Im[Z_{load}]$, which both decide about the amount of power leaving the engine and by extension of the engine's efficiency. However, the relation of power and efficiency is not linear, because an alteration of load impedance influences the amount of acoustic energy within the FBT.

3. THERMODYNAMIC ANALYSIS

3.1. Acoustic wave distribution

The result of numerical calculations is a plot of acoustic field distribution along the whole engine's loop, which is essential for an analysis of the engine performance. Fig. 2. presents the distribution of: (a) the amplitudes of pressure $|p_1|$ and the volume flow rate $|U_1|$, (b) normalized impedance Z_n and phasing φ and (c) acoustic power $\dot{E}$. Integration starts at position 0.5 m ahead of the centre of the regenerator, acoustic load is placed directly behind the core at x=0.75m and the stub is located at x=3.63m.

In the thermoacoustic core, one can see a growth of $|U_1|$ – caused by the thermoacoustic effect and a drop of $|p_1|$ – caused by viscous resistance. Due to the much enlarged core diameter, Z_n is clearly bigger and φ also rises in the direction of 0°. Both reach their targeted values in the middle of the REG. Hence, acoustic power is defined as:

$$\dot{E} = \frac{1}{2} \cdot \cos(\varphi) \cdot |p_1| \cdot |U_1|, \tag{3}$$

and it grows a lot in the core to be thereafter consumed mainly by acoustic load. Power consumption results in a fall of $|U_1|$ but it has almost no effect on other acoustic parameters.

In next part of the waveguide (FBT), φ oscillates between +/-10° and Z_n amounts to 1, which indicates very good travelling-wave conditions with only small standing-wave components. Viscous losses along FBT are rather small and acoustic power decreases only slightly. The stub then introduces a significant growth of φ and U_1. The acoustic wave between the stub and the core has a larger standing-wave component, which explains a higher drop of $\dot{E}$ in this section.

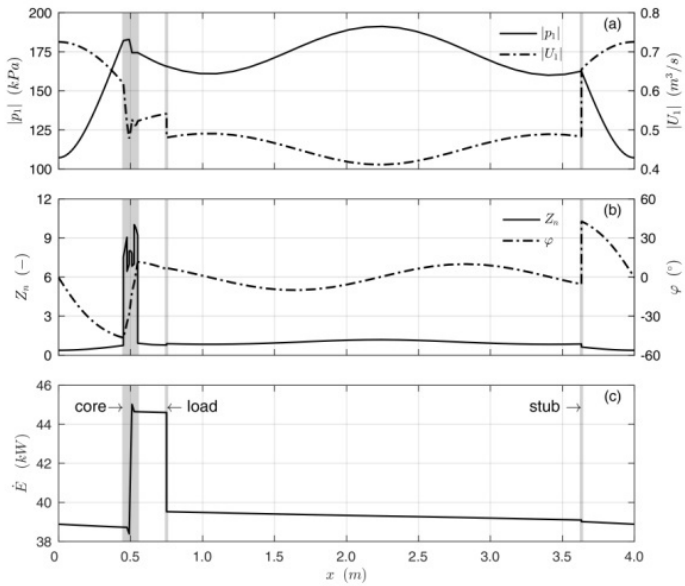

Fig. 2. Acoustic wave distribution along the engine's loop. (a) pressure $|p_1|$ and volume flow rate $|U_1|$ amplitudes, (b) phasing φ and normalized impe-dance Z_n, (c) acoustic power $\dot{E}$

3.2. Energy balance of the thermoacoustic engine

In the thermoacoustic engine, thermal energy is converted into acoustic one. Fig 1b. shows schematically the heat fluxes and acoustic power in the thermoacoustic system. Thermodynamic cycle occurs directly in the core, for which energy balance could be written as:

$$\dot{Q}_{HHX} - \dot{Q}_{AHX} - \dot{Q}_{diss} = \dot{E}_{ac,out} - \dot{E}_{ac,in}, \qquad (4)$$

where Q_{HHX} and Q_{AHX} are heat fluxes supplied in the hot heat exchanger (heater) and released in the ambient heat exchanger (cooler), $\dot{Q}_{diss}$ is heat loss in the core and ($\dot{E}_{ac,out}$- $\dot{E}_{ac,in}$) is an acoustic power gain in the core, which is basically the power of a thermodynamic cycle. Thermal efficiency is defined as:

$$\eta_{th} = \frac{\dot{E}_{ac,out} - \dot{E}_{ac,in}}{\dot{Q}_{HHX}}. \qquad (5)$$

The total efficiency of an engine can be derived considering load power $\dot{E}_{load}$ as a useful energy flux led out from the system, and it is defined as:

$$\eta = \frac{\dot{E}_{load}}{\dot{Q}_{HHX}}. \qquad (6)$$

A Carnot efficiency calculated by the definition:

$$\eta_{Carnot} = 1 - \frac{T_{AHX}}{T_{HHX}}, \qquad (7)$$

amounts to 31.9% for the assumed heater and cooler temperatures. In order to evaluate objectively the engine's performance, it is worth to compare efficiency relative to Carnot, known as exergetic efficiency. For the thermodynamic cycle and the whole device, it is defined in turn as:

$$\eta_{ex,th} = \frac{\eta_{th}}{\eta_{Carnot}} = \frac{\dot{E}_{ac,out} - \dot{E}_{ac,in}}{\dot{Q}_{HHX}\left(1 - \frac{T_{AHX}}{T_{HHX}}\right)}, \qquad (8)$$

$$\eta_{ex} = \frac{\eta}{\eta_{Carnot}} = \frac{\dot{E}_{load}}{\dot{Q}_{HHX}\left(1 - \frac{T_{AHX}}{T_{HHX}}\right)}. \qquad (9)$$

Fig. 3. presents energy balance of the whole thermoacoustic Stirling engine in the form of Sankey diagram. The darker colour denotes the balance of the thermal cycle. Out of 50.8 kW heat supplied in the hot heat exchanger 44.8 kW is taken out by the cold heat exchanger. The rest 6 kW reduced by a 0.1 kW heat loss in the core is the power of a thermal cycle, which means the exact acoustic power gain in the core. Acoustic energy balance is marked with a lighter colour.

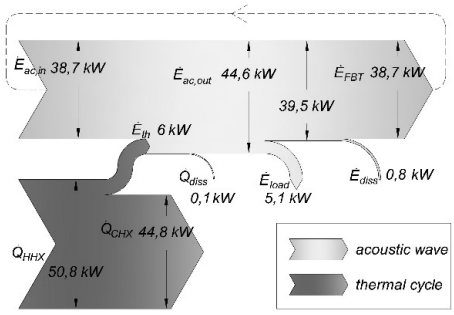

Fig. 3. Energy balance of analyzed thermoacoustic engine – Sankey diagram

The level of acoustic power in the FBT is very high in comparison to the power gain in the core. This is due to a relatively low temperature difference between the HHX and the AHX, which results in a low theoretical gain. Acoustic power entering the core amounts to 38.7 kW and due to the thermodynamic cycle it increases 1.15 times to the value of 44.6 kW. Thereafter, 5.1 kW leaves the system in the acoustic load and the rest 0.8 kW is dissipated because of viscosity and thermal relaxation along the FBT. In a steady state, 38.7 kW of acoustic power is transported around in the loop to drive the core again.

Introducing an acoustic load to the acoustic network is crucial for the parameters and performance of the engine. Fig 4. presents the influence of the load impedance on the engine power and efficiency. It should be noted that changing the value of $Re[Z_{load}]$ results in an automatic adjustment of the stub length and position in the simulation. It occurs in order to keep constant acoustic conditions in the REG (Z_n=8 and φ=-20°).

Without a load ($Re[Z_{load}] \rightarrow \infty$), acoustic power in the loop would grow up to the level where all the power gain is dissipated by the viscous losses in the FBT. Such a state is shown on the right side of the diagram, where the load power $\dot{E}_{load}$ and total exergetic efficiency is close to 0, while the cycle power $\dot{E}_{th}$ remains high. The ratio between the load power and the thermal cycle power is known here as the load efficiency:

$$\eta_{load} = \frac{\dot{E}_{load}}{\dot{E}_{th}} = \frac{\dot{E}_{load}}{\dot{E}_{ac,out} - \dot{E}_{ac,in}}, \qquad (10)$$

and depicted with a dotted line in the diagram.

A decrease of load impedance results in a steep rise of efficiency and power of the engine, however power reaches its maximum values for higher impedance than efficiency. Getting to the maximum of exergetic efficiency (ca. 40%) power is a few times lower than its maximum value. This discrepancy is caused by the fact that for lower power of the engine

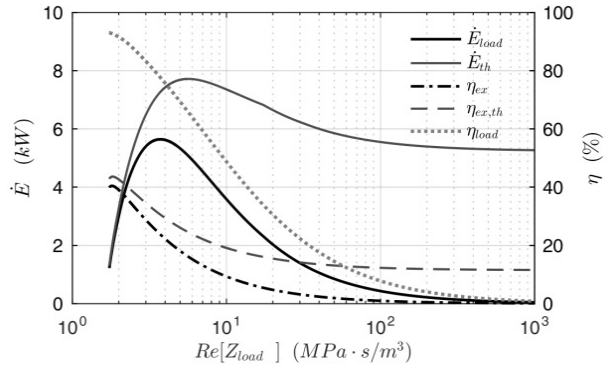

Fig. 4. Influence of the load impedance Re[Z_{load}] on engine power $\dot{E}_{load}$, thermal power of the thermodynamic cycle $\dot{E}_{th}$, exergetic total η_{ex} and thermal efficiency $\eta_{ex,th}$ and load efficiency η_{load}

(a lower acoustic power level), viscous losses decline significantly. Also, the temperature drop between the heat exchangers and theregenerator decreases slightly, which results in a bigger temperature difference over the regenerator. For both, reasons efficiency grows up. To suit the perfect load (characterised by impedance), one must find a trade-off between high efficiency and high power. The engine analysed in its basic state works with exergetic efficiency of 31% extracting 5.1 kW of power in the load.

4. CONCLUSIONS

The mathematical model of the thermoacoustic travelling-wave engine with a looped tube configuration was built with DeltaEC software. The main assumption was to supply the engine with a low-grade heat at the temperature of 150°C. In the article, the construction details of the engine are presented as well as its key parameters and the energy balance. The influence of load impedance on power and efficiency is deeply analysed. The maxima of power and efficiency are met for different impedance values, which means that an operating point should be optimised by a carefully chosen load. The Authors have proofed numerically that single-stage thermoacoustic engines could be used to utilise waste heat at 150°C with an exergetic efficiency in the range of 40%, however an experimental validation would be essential.

Nomenclature

Symbols

a – speed of sound, m/s
g – gain factor, 1/m
$\dot{E}$ – energy flow, acoustic power, W
L – length
p_1 – pressure oscillation, kPa
p_m – mean pressure, MPa
$\dot{Q}$ – heat flow, W
r_v – viscous resistance, Pa s/m^4
t – temperature, °C
T – temperature, K
U_1 – volumetric velocity, volume flow rate, m^3/s
X – position, cm
Z_n – normalized impedance, -
Z_{load} – acoustic impedance of the load, MPa s/m^3

Greek letters

η – efficiency, -
φ – phase difference between pressure and velocity oscillation, phasing, °
v_1 – velocity of the gas, m/s
ρ_m – mean density of the gas, kg/m^3

Acronyms

AHX – Ambient Heat Exchanger - cooler
FBT – Feedback Tube
HHX – Hot Heat Exchanger - heater
REG – Regenerator

References

1. Swift G.W. (2002), Thermoacoustics: A Unifying Perspective for Some Engines and Refrigerators, Acoustical Society of America.
2. Ceperley P.H. (1979), A pistonless Stirling engine -The traveling wave heat engine, *J. Acoust. Soc. Am*. 66, 1508–1513.
3. Ceperley P.H. (1985), Gain and efficiency of a short traveling wave heat engine, *J. Acoust. Soc. Am*. 77, 1239–1244.
4. Yazaki T., Iwata A., Maekawa T., Tominaga A. (1998), Traveling Wave Thermoacoustic Engine in a Looped Tube, *Phys. Rev. Lett*. 81, 3128–3131.
5. Backhaus S., Swift G.W. (2000), A thermoacoustic-Stirling heat engine: detailed study, *J. Acoust. Soc. Am*. 107, 3148–66.
6. Tijani M.E.H., Spoelstra S. (2011), A high performance thermoacoustic engine, *J. Appl. Phys*. 110, 93519.
7. Haberbusch M.S., Nguyen C.T., Ickes J.C., Hui T.Y. (2013), 4 kW Thermoacoustic Stirling Heat Engine Test Results, 11th Int. Energy Convers. Eng. Conf., San Jose.

8. de Blok K. (2008), Low operating temperature integral thermo acoustic devices for solar cooling and waste heat recovery, *J. Acoust. Soc. Am.* 123, 3541.
9. Zhang X., Chang J., Cai S., Hu J. (2016), A multi-stage travelling wave thermoacoustic engine driven refrigerator and operation features for utilizing low grade energy, *Energy Convers. Manag*. 114, 224–233.
10. de Blok K. (2012), Multi-stage Traveling Wave Thermoacoustics in Practice, in: ICSV 19, Vilnius, Lithuania, 2012, pp. 1–8.
11. Zhang X., Chang J. (2015), Onset and steady-operation features of low temperature differential multi-stage travelling wave thermoacoustic engines for low grade energy utilization, *Energy Convers. Manag*. 105, 810–816.
12. Ward B., Clark J.; Swift G.W. (2016), Design environment for low-amplitude thermoacoustic energy conversion (DeltaEC), Version 6.4b2, Users Guide, E-Book.
13. Yu Z., Jaworski A.J. (2010), Impact of acoustic impedance and flow resistance on the power output capacity of the regenerators in travelling-wave thermoacoustic engines, *Energy Convers. Manag*. 51, 350–359.
14. Bi T., Wu Z., Zhang L. (2015), Yu G., Luo E., Dai W., Development of a 5kW traveling-wave thermoacoustic electric generator, *Appl. Energy*, 1–7.
15. Wang K., Zhang J., Zhang N., Sun D.,. Luo K, Zou J., Qiu L. (2016), Acoustic matching of a traveling-wave thermoacoustic electric generator, *Appl. Therm. Eng*. 102, 272–282.
16. Backhaus S., Tward E., Petach M. (2004), Traveling-wave thermoacoustic electric generator, *Appl. Phys. Lett*. 85, 1085–1087.
17. de Blok K., Owczarek P., Francois M. (2014), Bi-directional turbines for converting acoustic wave power into electricity, 9th PAMIR Int. Conf., Ryga.
18. Kruse, A., Ruziewicz, A., Tajmar, M., Gnutek, Z. (2017), A numerical study of a looped-tube thermoacoustic engine with a single-stage for utilization of low-grade heat. *Energy Conversion and Management*, 149, 206–218.

Biographical notes

Adam Ruziewicz received his M.Sc. degree in Power Engineering with the following specialization: Renewable Energy Sources at the Faculty of Mechanical and Power Engineering at the Wroclaw University of Science Technology. Currently, he studies further in the same faculty as a PhD candidate carrying out research on thermoacoustic systems. Since 2017, he has been working as a research-didactic assistant at the Department of Thermodynamics, Theory of Machines and Thermal Systems. His main scientific interests include thermoacoustic devices and their possible applications including waste and solar heat utilisation.

Alexander Kruse studied mechanical engineering at TU Dresden with the special field of aerospace engineering. He obtained his Dipl.-Ing.'s degree after researching waste heat utilization with thermoelectric generators for space applications. He graduated in 2012. That same year he started working as a PhD student at the Institute of Aerospace Engineering, TU Dresden, and the Boysen-TU Dresden-Graduiertenkolleg (a doctorate program). He is currently engaged in numerical and experimental research on single- and multi-stage thermoacoustic engines for waste heat recovery applications.

Zbigniew Gnutek received his PhD degree in 1977 at the Department of Thermodynamics at the Wroclaw University of Science and Technology, and the same year he became an assistant professor in the same department. In 1997, he received D.Sc. and in 2005 he was conferred on Professor degree. The field of his scientific interests is in general the theory of machines and thermal devices which concerns the problems of cryogenics, volume machines, as well as energy conversions systems. He is also engaged with renewable and waste heat sources and the ORC power generators. He is an author or co-author of 175 scientific publications including 5 books and 1 script. He promoted 11 PhD candidates and was a reviewer for 18 PhD, 4 D.Sc. and 4 Professor promotions. He is currently the Dean of the Faculty of Mechanical and Power Engineering.